U-RANS simulation of mixed-convection around a finite wall-mounted heated cylinder cooled by cross-flow

Yannick Lecocq, Sophie Bournaud, Remi Manceau, Bernard Duret, Laurent-Emmanuel Brizzi

U-RANS SIMULATION OF MIXED-CONVECTION AROUND A FINITE WALL-MOUNTED HEATED CYLINDER COOLED BY CROSS-FLOW

Y. Lecocq
EDF R&D, Dept. MFEE, 6 Quai Watier BP 49
F-78401 Chatou Cedex – France
Ph. 33 (1) 30 87 86 61-Fax 33 (1) 30 87 74 61
yannick.lecocq@lea.univ-poitiers.fr

S. Bournaud
EDF R&D, Dept. MFEE, 6 Quai Watier BP 49
F-78401 Chatou Cedex – France
Ph. 33 (1) 30 87 86 61-Fax 33 (1) 30 87 74 61
sophie.bournaud@edf.fr

R. Manceau
LEA, Université de Poitiers,
ENSMA, CNRS, France
remi.manceau@lea.univ-poitiers.fr

B Duret
LTGD CEA Grenoble France
bernard.duret@cea.fr

L. Brizzi
LEA, Université de Poitiers,
ENSMA, CNRS, France
laurent.brizzi@lea.univ-poitiers.fr

ABSTRACT

VALIDA experiments [1] were carried out within the framework of radioactive waste management to improve the understanding of mixed-convection flow and more particularly the interaction between a global cross-flow circulation and local natural convection effects around a vertical heated cylinder. The VALIDA loop implements a cylinder of 3.1 height to diameter ratio, mounted vertically in an insulated tunnel and cooled by a cross-flow air circulation.

The air flow and the temperature fields on the cylinder and in the plume behind it have been numerically studied using Unsteady Reynolds Average Navier Stokes simulation (U-RANS) and compared to experimental data. The purpose of this paper is to present the results of a k-ω SST model on several test cases. The numerical tools used herein are *Code_Saturne,* EDF finite volume CFD code [2], and *Syrthes*, EDF finite element code for solid temperatures [9]. For the studied test-cases, Reynolds and Grashof numbers are characteristic of a sub-critical flow regime with laminar boundary layers around the cylinder and a turbulent wake. From the transient downstream air calculations, the plume behind the cylinder and its wall temperatures are analysed and compared to experimental data. The flow pattern strongly depends on the ratio of the buoyancy to the inertia force. Results show satisfactory qualitative and quantitative behaviour.

NOMENCLATURE

h	$[W/m^2°C]$	Heat transfer coefficient
Φ	$[W/m^2]$	Heat flux density
Φ_V	$[W/m^3]$	Total power (source or sink)
V	$[m.s^{-1}]$	Mean air velocity
$\bar{u}$	$[m.s^{-1}]$	Instantaneous air velocity
$\vec{g}$	$[m.s^{-2}]$	Gravity vector
D	$[m]$	Cylinder diameter
H	$[m]$	Cylinder height
P	$[Pa]$	Air pressure
t	$[s]$	Time
T	$[°C]$	Temperature
T_0	$[°C]$	Reference temperature
ρ	$[kg/m^3]$	Density
β	$[1/K]$	Thermal expansion coefficient
μ	$[kg/(m.s)]$	Dynamic viscosity
ν	$[m^2.s^{-1}]$	Kinematic viscosity
C_p	$[J/(kg.K)]$	Specific heat
λ	$[W/m/K]$	Thermal conductivity
Re	[–]	Reynolds number
Gr*	[–]	Grashof number: $g\,\beta\,H^4\,\Phi\,/(\nu^2\lambda)$
Ri	[–]	Richardson number
St	[–]	Strouhal number

Keywords : finite circular cylinder, cross-flow cooling, heat transfer, U-RANS, mixed-convection

INTRODUCTION

Within the framework of radioactive waste management, the VALIDA program started to provide reliable experimental data for the validation of numerical tools utilized to model the cooling of spent nuclear fuel containers in dry storage facilities. The design of such facilities implies thermal-aeraulic calculations in order to predict containers and wall temperatures. These temperatures must never exceed critical values. The understanding of mixed-convection flow and more particularly the interaction between a global cross-flow circulation and local natural convection effects is a key point of these design studies. VALIDA experiments [1] were carried out for this purpose at CEA on a finite circular heated cylinder of 3.1 height to diameter ratio, mounted vertically in an insulated tunnel and cooled by a cross-flow air circulation.

This paper introduces the main experimental results obtained in the VALIDA configuration [1] and uses the corresponding LES simulations [3]. Steady-state cylinder and air temperature measurements are then compared to U-RANS computations using a k-ω-SST model implemented within EDF CFD tool *Code_Saturne* [4]. For the test cases studied, the air input velocity is varied from 0.25 to 1m.s^{-1} and the heat flux on the cylinder wall from 330 to 850 W.m^{-2}. Hence, Reynolds numbers based on the cylinder diameter are $11\,000 < Re < 43\,000$ and Grashof numbers $3.0\ 10^{10} < Gr^* < 2.4\ 10^{12}$.

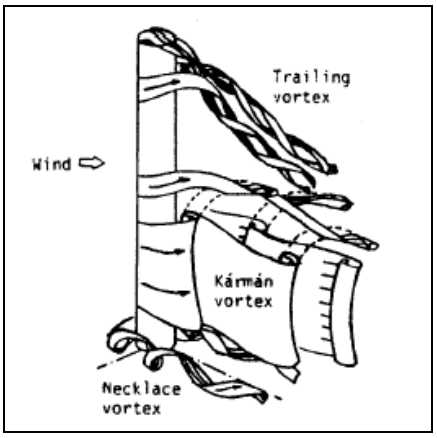

Figure 1 : Typical isothermal flow structures

VALIDA CONFIGURATION

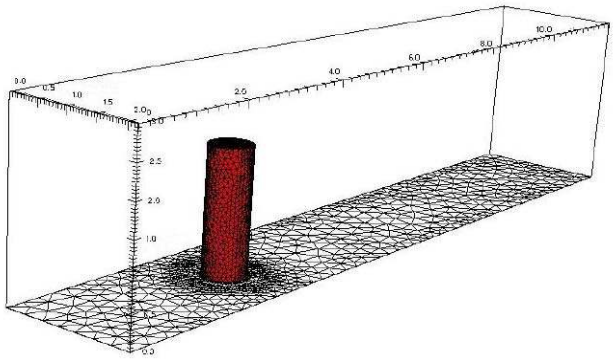

Figure 2 : View of VALIDA configuration

Experimental set-up

The heated cylinder investigated in the present work is that from the experiments by Duret et al. [1] [5]. The geometry of the computational domain is given in Figure 2.

Located at CEA, the VALIDA loop implements a cylinder of 3.1 height to diameter ratio: H=2 m and D=0.64 m. It is mounted vertically in an insulated tunnel and cooled by a cross-flow air circulation. The wind tunnel is a rectangular–shaped channel with a 2.14 m width, 3 m height, and a 12 m length from inlet to outlet. The cylinder axis is placed in the middle of the channel width, at 3 m from the inlet (see Figure 2). The two lateral walls are therefore at a distance of 0.75 m from the cylinder wall.

Experimental test cases

A constant heat flux density Φ is imposed at the inner face of the lateral and top walls of the cylinder, which are 5.10^{-3} m thick.

Six test cases have been performed, for V_{air}=0.25, 0.5 and 1m.s^{-1}and Φ=330, 600 and 850 W.m^{-2} Table 1 gives the experimental input data simulated for the test cases presented herein, and their associated dimensionless numbers: Reynolds number Re, Grashof number Gr* and Richardson number Ri. The Richardson number represents a ratio of the upwelling forces to the inertial forces. In this regard, it can be considered as a $(U_{cn}/U)^2$ ratio, U_{cn} being the characteristic velocity due to natural convection and U the transverse velocity.

Test case name Flux ($W.m^{-2}$) Inlet velocity($m.s^{-1}$)	Re	Gr*	Ri
Φ=330 V=1	43000	$3.0\ 10^{10}$	4
Φ=600 V=1	**43000**	**$6.7\ 10^{10}$**	**6**
Φ=850 V=1	43000	$1.2\ 10^{11}$	8
Φ=850 V=0.75	32000	$2.0\ 10^{11}$	14
Φ=850 V=0.5	21000	$5.1\ 10^{11}$	34
Φ=850 V=0.25	11000	$2.4\ 10^{12}$	140

Table 1 : Experimental input parameters

Air and cylinder temperature measurements are described in details in [1]. The air temperature is measured behind the cylinder, using a movable frame with 77 thermocouples. The cylinder wall temperatures are measured along an instrumented vertical line which can be placed at different angular locations by rotating the cylinder. A temperature measurements accuracy of ±0.5°C can be considered. The test "Φ=600 $W.m^{-2}$ V=1 $m.s^{-1}$ " is considered the reference test-case hereafter.

Mathematical formulation

Continuous equations

Conservation equations for mass, momentum and energy of the fluid flow are given in differential form by using the Einstein summation. Navier-Stokes equations can be written as follows (1):

$$\begin{cases} \dfrac{\partial}{\partial x_j}(\rho u_j) = 0 \\ \dfrac{\partial}{\partial t}(\rho u_i) + \dfrac{\partial}{\partial x_j}(\rho u_i u_j) = -\dfrac{\partial}{\partial x_i}P + \dfrac{\partial}{\partial x_j}\tau_{ij} + g_i\delta\rho \\ \dfrac{\partial}{\partial t}(\rho T) + \dfrac{\partial}{\partial x_j}(\rho u_j T) = \dfrac{\partial}{\partial x_j}\left[\left(\dfrac{\lambda}{Cp}\right)\dfrac{\partial T}{\partial x_j}\right] \end{cases}$$

In the above equations (1), T is the temperature, λ the fluid conductivity, c_p the specific heat. $\underline{\underline{\tau}}$ stands for the viscous stress tensor with:

$$\underline{\underline{\tau}} = 2\mu\underline{\underline{D}} - \frac{2}{3}\mu \times tr(\underline{\underline{D}})\underline{\underline{Id}}$$

$$\underline{\underline{D}} = \frac{1}{2}(\underline{\underline{grad}}(\bar{u}) + {}^{t}\underline{\underline{grad}}(\bar{u}))$$

μ represents the dynamic molecular viscosity.

Reynolds averaged equations

In case of turbulence, the equations have to be averaged. The Reynolds decomposition of variables in mean and fluctuating parts is applied to velocity, pressure and temperature. The statistical approach to turbulence, applied to (1) produces the following system:

$$\begin{cases} \dfrac{\partial}{\partial x_j}(\rho\overline{u_j}) = 0 \\ \dfrac{\partial}{\partial t}(\rho\overline{u_i}) + \dfrac{\partial}{\partial x_j}(\rho\overline{u_i}\,\overline{u_j}) = -\dfrac{\partial}{\partial x_i}\overline{p} + \dfrac{\partial}{\partial x_j}\overline{\tau_{ij}} - \dfrac{\partial}{\partial x_j}(\rho\overline{u_j'u_i'}) + g_i\delta\rho \\ \dfrac{\partial}{\partial t}(\rho\overline{T}) + \dfrac{\partial}{\partial x_j}(\rho\overline{u_j}\,\overline{T}) = \dfrac{\partial}{\partial x_j}\left[\left(\dfrac{\lambda}{Cp}\right)\dfrac{\partial\overline{T}}{\partial x_j}\right] - \dfrac{\partial}{\partial x_j}(\rho\overline{u_j'T'}) \end{cases}$$

The Reynolds stress tensor $\overline{u_j'u_i'}$ and the turbulent heat flux $\overline{u_j'T'}$ have appeared in the averaging process. They represent new unknown terms. To close the system, turbulence correlations need to be modelled.

It is worth noting that in the present study, the flow is considered incompressible, but the density varies as a function of the mean temperature.

Turbulent heat flux

Turbulent heat flux is modelled in *Code_Saturne* by a simple gradient hypothesis:

$$\overline{u_j'T'} = -\left[\left(\frac{\nu_t}{\rho\ \mathrm{Pr}_t}\right)\frac{\partial\overline{T}}{\partial x_j}\right]$$

where Pr_t is the turbulent Prandtl number and υ_t the turbulent viscosity

Turbulence model

The SST turbulence model used in the present study is based on a linear constitutive equation for the Reynolds stress $\overline{u_j'u_i'}$

$$\overline{u_j'u_i'} = -\upsilon_t\left(\frac{\partial\overline{u_i}}{\partial x_j} + \frac{\partial\overline{u_j}}{\partial x_i}\right) + \frac{2}{3}k\delta_{ij}$$

where k stands for the turbulent kinetic energy, and δ_{ij} is Kronecker's symbol.

The SST model (Menter [4]) is a hybrid k - ε /k - ω model, designed in order to combine the strength of the two models: the ability of the k - ω model proposed by Wilcox [6] to reproduce boundary layers and separation, the ability of the k - ε model (Jones and Launder [16]) to reproduce free-shear flows and its independence of the arbitrary free-stream boundary conditions.

The model is built using a blending function, which appears as a coefficient in the equation, in order to progressively switch from the ε equation to the ω equation when the wall is approached. Additional features of the SST model is a limiter on the eddy viscosity to avoid an overestimation in the near-wall region and a production limiter to get rid of the overproduction of turbulent kinetic energy at stagnation points. The equations for SST model are [6]:

$$\begin{cases} \dfrac{\partial \rho k}{\partial t} + \dfrac{\partial \rho k \overline{u_j}}{\partial x_j} = \mu_t \left(\dfrac{\partial \overline{u_i}}{\partial x_j} + \dfrac{\partial \overline{u_j}}{\partial x_i} \right) \dfrac{\partial \overline{u_i}}{\partial x_j} + \dfrac{\partial}{\partial x_j} \left(\dfrac{\mu_t}{\sigma_k} \dfrac{\partial k}{\partial x_j} \right) - \beta \rho \omega k \\ \dfrac{\partial \rho \omega}{\partial t} + \dfrac{\partial \rho \omega \overline{u_j}}{\partial x_j} = -\alpha \rho \dfrac{\omega}{k} \overline{u_i' u_j'} \dfrac{\partial \overline{u_i}}{\partial x_j} + \dfrac{\partial}{\partial x_j} \left(\sigma \mu_t \dfrac{\partial \omega}{\partial x_j} \right) - \beta \rho \omega^2 \end{cases}$$

$$\alpha = \frac{5}{9}; \beta = \frac{3}{40}; \sigma = \frac{1}{2}; \sigma_k = 1$$

Numerical tool description

EDF CFD tool *Code_Saturne*

The EDF in-house finite volume CFD tool *Code_Saturne* [2] is used to solve Navier-Stokes equations on unstructured meshes. The code is based on an unstructured and collocated approach that handles cells of any shape. Air is assumed incompressible but density and viscosity are functions of the mean temperature.

The momentum equations are solved by considering an explicit mass flux. The three components of the velocity are thus uncoupled. Velocity and pressure coupling is insured by a SIMPLEC prediction/correction method [7]. The Poisson equation is solved with a conjugate gradient algorithm with diagonal preconditioning. The collocated discretisation requires a Rhie and Chow interpolation [8] in the correction step to avoid oscillatory solutions. This interpolation has been used in the present application, although it doesn't seem essential for unstructured meshes.

Solid Code *Syrthes*

The solid code *Syrthes* [9] is coupled with *Code_Saturne* to compute the cylinder temperature. It uses a finite element technique to solve the following general heat equation where all properties can be time, space or temperature dependent.

$$\rho C_p \frac{\partial T}{\partial t} = \frac{\partial}{\partial x_j} \left(k_s \frac{\partial T}{\partial x_j} \right) + \Phi_v$$

T is the temperature, Φ_v a volumic source or sink, ρ and C_p, respectively the density and the specific heat.

More details on the possibilities of the finite element code *Syrthes* can be found in [9]. Like *Code_Saturne*, *Syrthes* has been checked thoroughly against experimental and analytical test cases proving that it gives very accurate solutions in problems similar to the present one.

Heat transfer at the solid / air interface

The thermal coupling between each code at each face of the air/solid interface is based, at every time step, on the exchange of the wall temperature from *Syrthes* to *Code_Saturne*. The exchange coefficient h defining the heat flux at the wall is thus calculated by *Code_Saturne* and returned to *Syrthes*. Then, the two codes work separately and calculate their own temperature implicitly considering the same heat flux. In order to accelerate convergence, the time-step for *Syrthes* computations can be taken different from *Code_Saturne*'s one, which basically corresponds to temporarily increase the conductivity of the solid material.

Let T_s be the temperature of the solid node at the interface, and T_f the temperature of the corresponding first node in the fluid domain (note that there is no need of conformity between the solid and the fluid meshes). At the beginning of the time step n, *Code_Saturne* receives from *Syrthes* the value of Ts_n and uses it to calculate the exchange coefficient h_n, defining the heat flux at the wall by $\varphi=h(T_s-T_f)$ and sends it to *Syrthes*. Then, the two codes run separately. *Code_Saturne* calculates Tf_{n+1} implicitly considering the heat flux $\varphi_{n+1}=h_n(Ts_n-Tf_{n+1})$ whereas *Syrthes* calculates Ts_{n+1}, also implicitly, considering the flux $\varphi_{n+1}=h_n(Ts_{n+1}-Tf_n)$. The system is then ready to perform the next time step.

Meshes

The calculation presented here is used to qualify *Code_Saturne* calculations for the cooling of spent nuclear fuel containers in dry storage facilities. The investigated phenomena are occurring around and behind the cylinder, in the plume. Due to the coupled resolution of heat conduction in the heating cylinder and the high Reynolds number convection of cooling air around it, fine meshes are required in and around the cylinder to simulate such thermal interactions and mixing phenomena which are affected by the processes in the boundary layers. For the present calculations, millimetric mesh sizes are thus used in and close to the cylinder to resolve the boundary layers down to the wall. The fluid mesh is presented in Figure 4. It contains 835.000 cells and gives a maximum non-dimensional distance to the wall of 7. The *Syrthes* solid mesh is presented in Figure 3. It contains 73 000 tetrahedra.

Numerical parameters

Input data and boundary conditions

In this specific study, the inlet air velocity is 0.25, 0.5 or 1ms^{-1} with uniform profile in space and constant in time. The inlet turbulent intensity $I_t = \frac{\upsilon_t}{\upsilon}$ taken into account is 2 %, in accordance with the experiments. The physical properties of the air fluid and steel cylinder are set temperature dependant with a Sutherland evaluation. The uniform heat flux density imposed on the inner face of the cylinder wall, including cover is Φ (W.m^{-2}).

Zero gradients are imposed as free boundary conditions at the channel outlet for temperature and velocity. Adiabatic and frictional conditions are used for ground and roof. Symmetry conditions are taken into consideration on lateral walls, in order to avoid having to refine the mesh to solve the boundary layer.

Initial thermal calculation process

Due to the weighty thermal inertia of the solid cylinder compared to thermal air evolutions, a specific pre–calculation process is needed to accelerate the thermal solid convergence. This process is carried out in two steps:

- a first calculation of the air is made around a cylinder doted with an artificial inertia, intentionally lowered in order to achieve typical steady average air velocity and solid temperature fields,
- then, a *Syrthes*-coupled calculation is done.

It should be noted that during the real fluid/solid calculation, cylinder's temperature field is not significantly modified, i.e., the thermal inertia of the cylinder is such that its temperature is not able to follow the frequencies imposed by the flow.

COMPUTATIONAL RESULTS

Qualitative observations

The field covered in VALIDA is characteristic of a sub-critical transverse convection regime shown in Figure 1. For the reference test-case, the Reynolds number, based on the cylinder diameter, the bulk air velocity, and the reference viscosity, is Re ~ 43 000, therefore between 10^3 and 2.10^5 (sub-critical regime). Such a regime is characterized by laminar boundary layers, laminar flow separation, transition in the separated shear-layer and regular alternate vortex shedding (Zukauskas [10], Williamson [11]).

Laminar boundary layers develop from the stagnation point on the cylinder. Inside these boundary layers, pressure is approximately constant along the radius of the cylinder.

On the contrary, tangentially to the wall, air velocity increases along the front face from the stagnation point, and then decreases along the rear face. When the wall-normal velocity gradient equals zero, the boundary layer separates from the wall and convection heat exchanges reach a minimum. The separated flow area at the back of the cylinder appears to be turbulent. This general flow behaviour is well observed in computations. Examples are given in Figure 5. The figures show instantaneous temperature fields in several planes. Karman vortices appear very clearly in the plane z = 3H/2. The effect of natural convection behind and very close to the wall cylinder may also be pointed out through these figures.

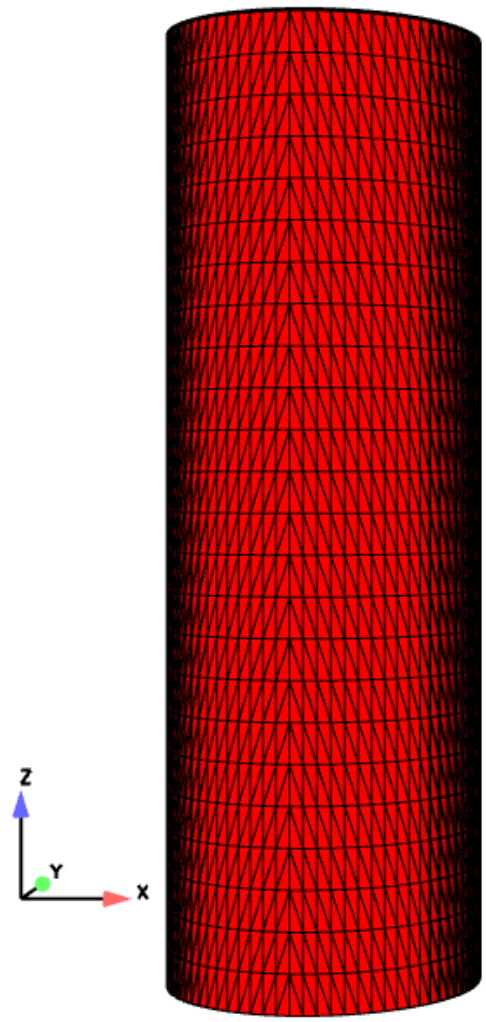

Figure 3: Meshing of the VALIDA test cylinder used for *Syrthes*

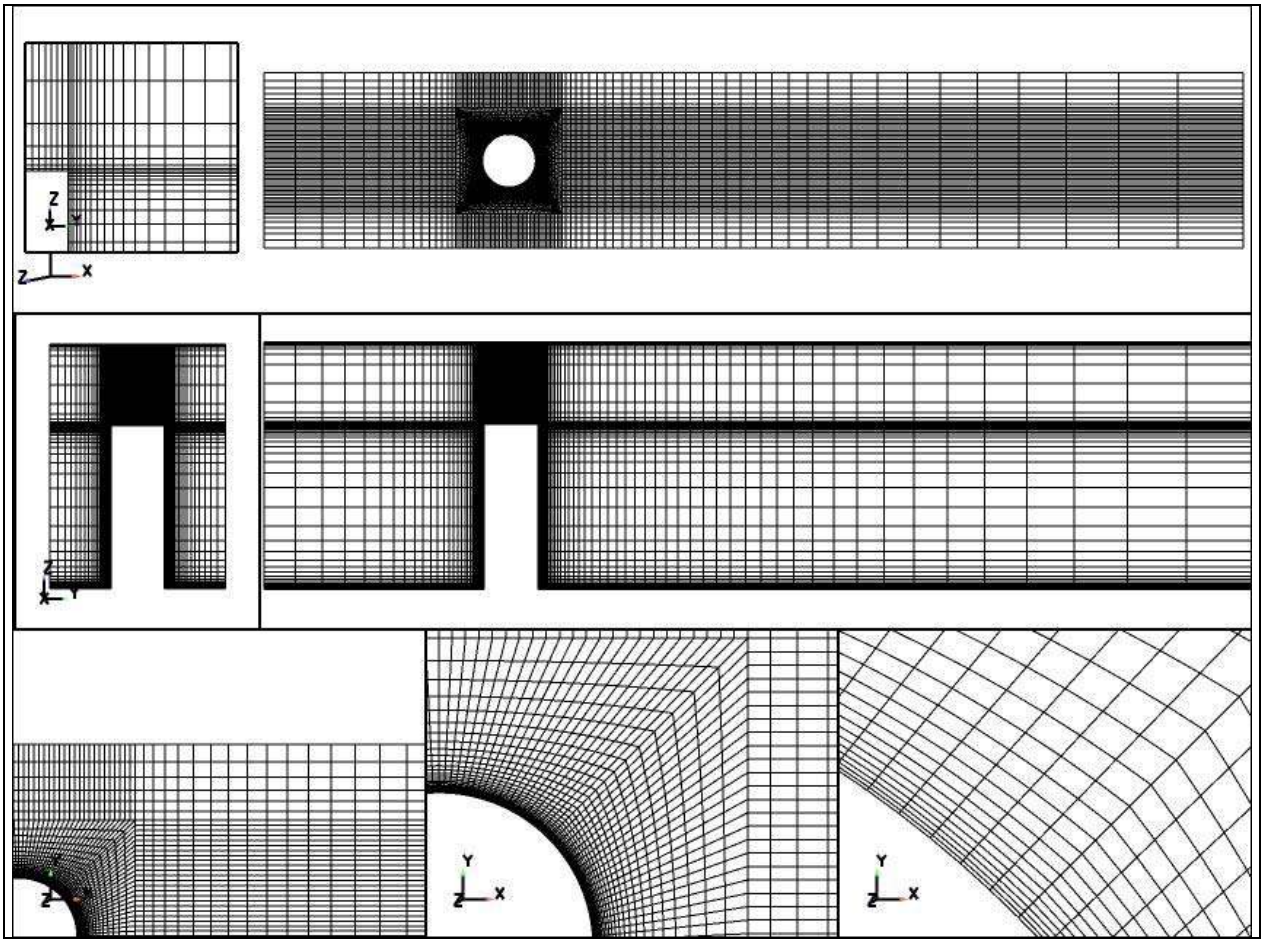

Figure 4: Meshing of the VALIDA test facility used for *Code_Saturne*

Instantaneous signal analyses

For the present calculations, the time-step is set to 10^{-3} s, giving a maximum CFL number of 4.

FFT Fourier transforms of longitudinal air velocity signal in the wake of the cylinder determine a characteristic frequency of $f_0 = 0.3$ Hz. This characteristic frequency corresponds to a Strouhal number St of 0.2 where $St = f_0.D/V$ with D the cylinder diameter and V the bulk air velocity ($1ms^{-1}$), see Figure 9. This Strouhal number is related to the Strouhal number of shedding vortices commonly observed [12] for a circular cylinder immersed in a steady cross flow in the range $10^4 < Re < 10^5$. Karman vortices appears quite significantly at $z = 3H/2$ except for $Ri = 140$, see Figure 5.

COMPARISON WITH EXPERIMENTS

Statistics have been collected during about 200 s. The averaging starts at $t = 120$ s and lasts more than fours tunnel flow-through. Experimental and computed results for air temperatures behind the cylinder are qualitatively compared in Figure 8. Figure 10 compares them quantitatively. Experimental and computed results for the cylinder temperatures are qualitatively compared in Figure 7. Figure 11 compares them quantitatively. In Figure 10, LES results [3] are also shown, as well as computations made using the SSG Reynolds-stress model [17] with wall functions (with a mesh without near-wall refinement). Results obtained with the SST model with a coarser mesh (MG) are also included to provide some indication about grid convergence.

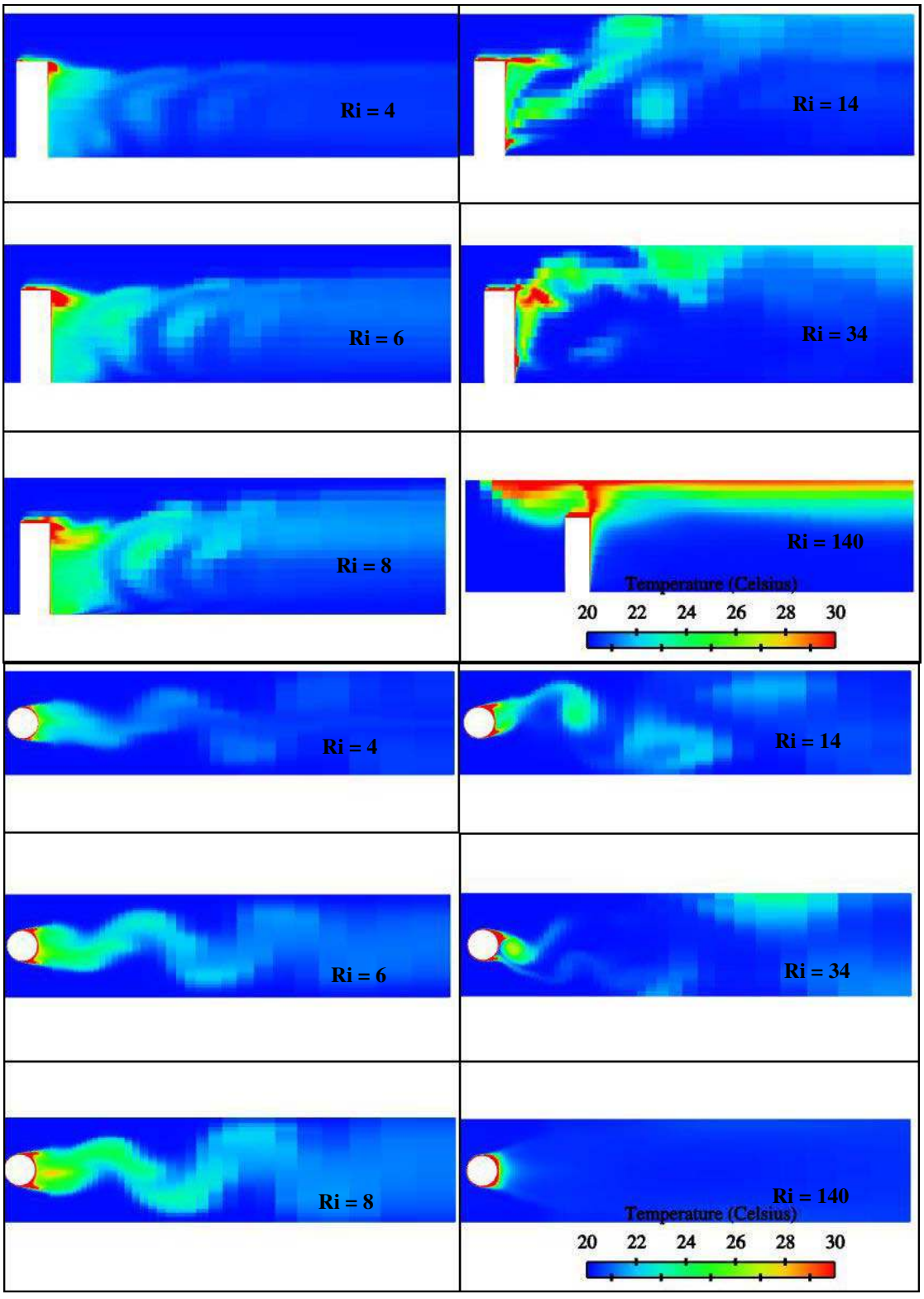

Figure 5: Instantaneous air temperatures in the longitudinal middle cut–plane and in the horizontal cut-plane at z = 3H/2

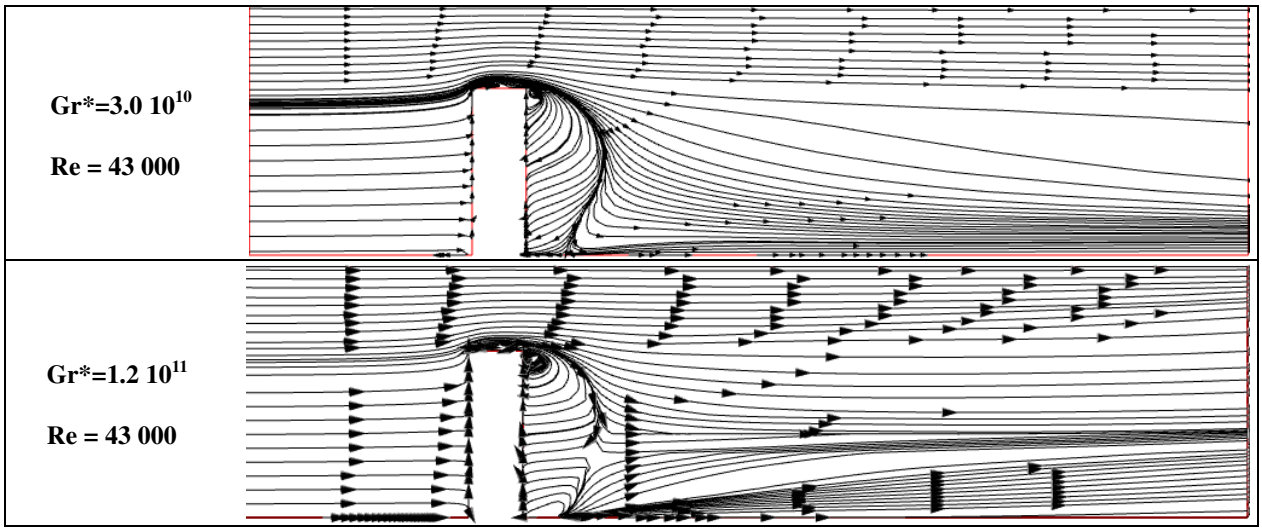

Figure 6: Air stream lines for Re = 43 000 and two different Gr* numbers - Gr*=3.0 10^{10} and Gr*=1.2 10^{11}

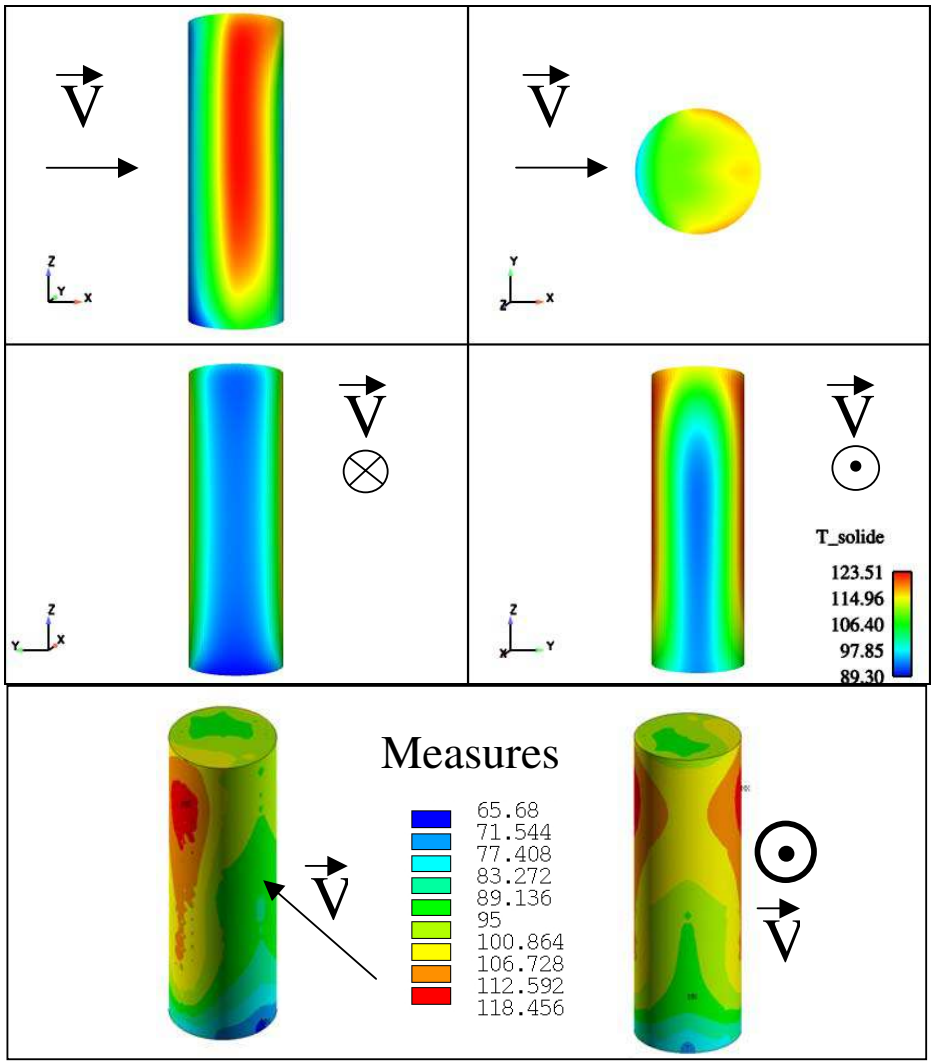

Figure 7 : Experimental and computed cylinder temperatures for the reference test-case

The overall agreement is satisfactory. In Figure 10, at z = H/4, the discrepancies between all the computations and the experiments is to be related to an insufficient insulation of the ground in the experimental facility. At z = 3H/4, the importance of resolving the near-wall region clearly appears. At z = H, the underestimation of the temperature by the SST model can be attributed to a slightly too strong downwash behind the top of the cylinder, which brings cool air from the region above the cylinder.

The wall temperatures shown in Figure 11 are very satisfactory, again taking into account the fact that the experimental temperatures are underestimated in the region close to the ground due to the heat leakage.

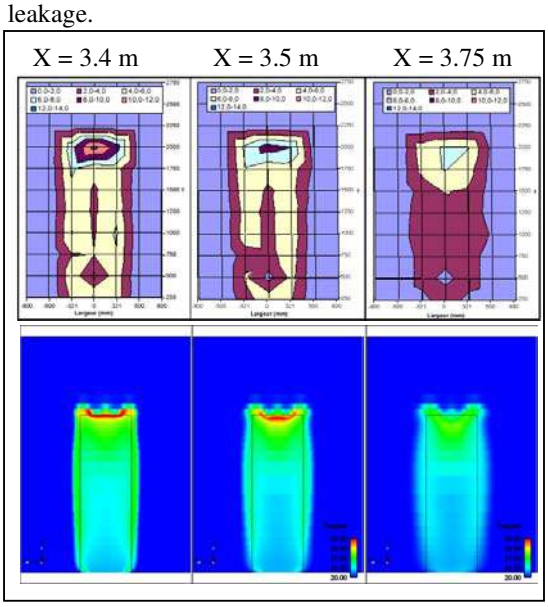

Figure 8: Experimental and computed air temperature behind the cylinder for the reference test-case

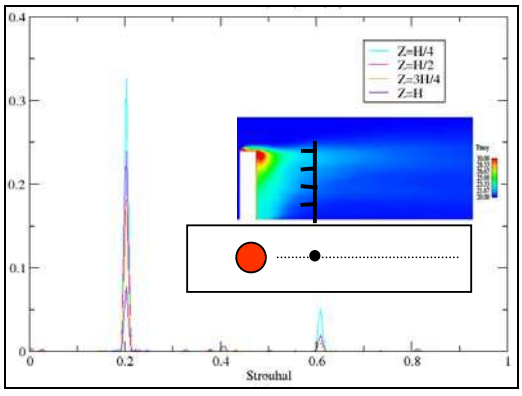

Figure 9: Air velocity FFT

CONCLUSION AND PERSPECTIVES

VALIDA experiments were carried out at CEA on a heated cylinder, vertically mounted in a dedicated wind tunnel. During the experiments, the air flow, the velocity profile and the heating power have been controlled and adjusted to simulate various thermal-hydraulic conditions. Test-cases involve varied Re and Gr* numbers.

Numerical simulations using a k - ω U-RANS model were performed on the experimental configuration to study the air flow and temperature fields on the cylinder and in the plume. They show different flow regimes, for the different experimental inputs tested ; Test cases where experimental convective transfers involve predominately forced or natural convection are distinguished thanks to established temperature maps. Numerical results have been compared to experimental results. Main comparisons between computations and measures show good agreement and satisfactory qualitative temperature distributions in the air and upon cylinder surface.

The velocity field observed in the reference test-case is characteristic of a sub-critical transverse convection regime with Re ~ 43 000. Karman vortices appear very clearly for this test-case in the computational results. Their characteristic frequency corresponds to the Strouhal number of shedding vortices commonly observed for a circular cylinder immersed in a steady cross flow.

This qualification can lead to local heat transfer estimations. Related to the considered upwind, lateral or downstream edges of the cylinder, these estimations might open out into the establishment of correlations for heat transfer coefficient in mixed convection [13].

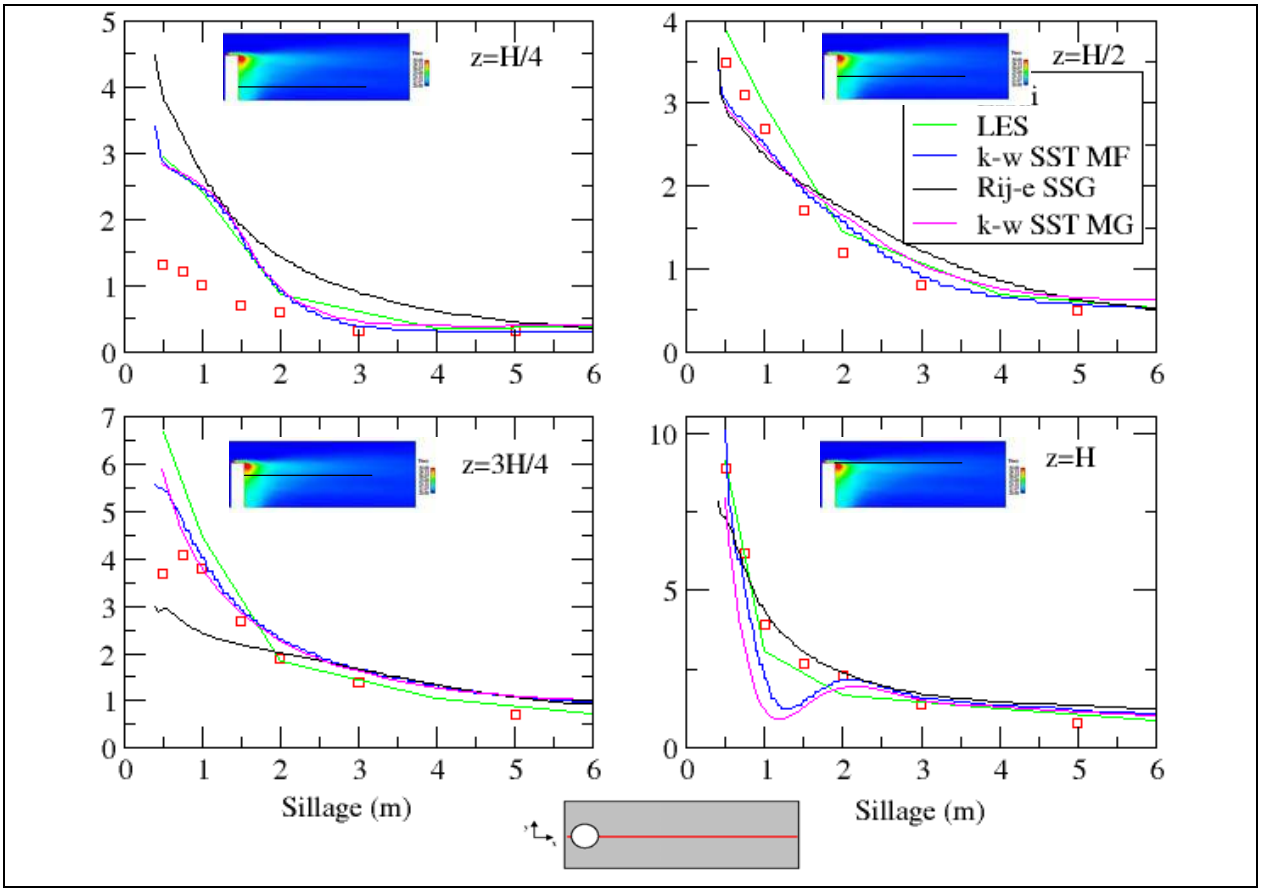

Figure 10: Experimental and computed relative air temperature T_r (°C) behind the cylinder - $T_r=T-T_0$

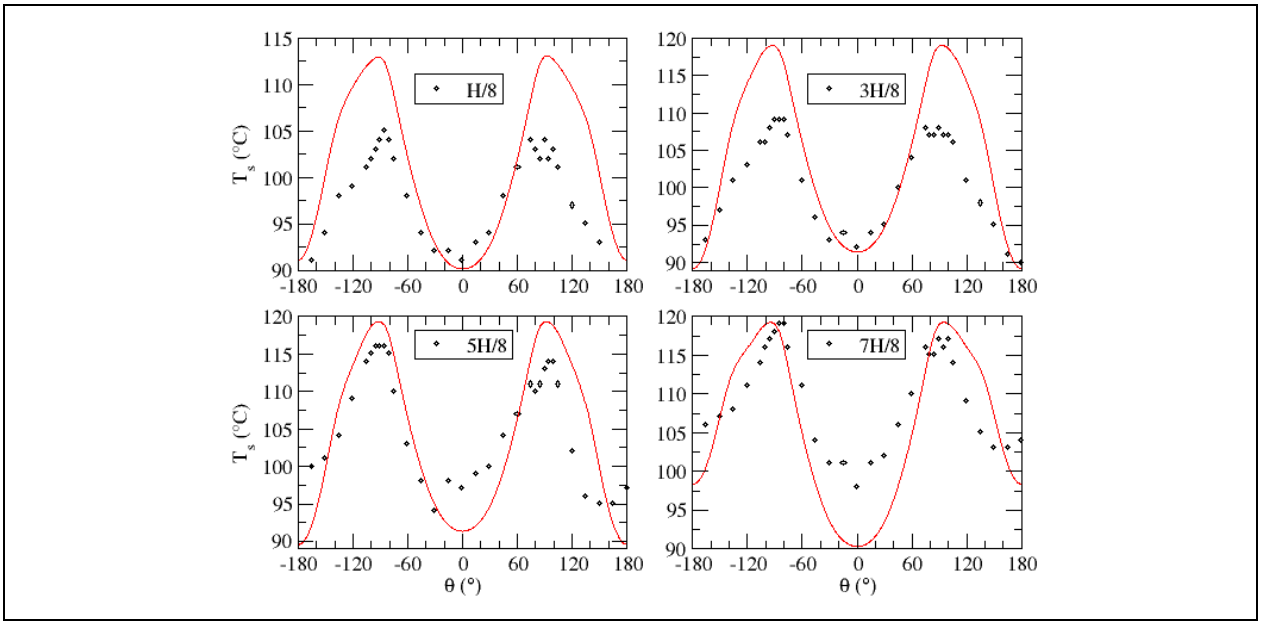

Figure 11: Experimental and computed cylinder temperatures for the reference test-case

REFERENCES

[1] Duret, B., Bonnard, JC., Chataing, T., Colmont, D., VALIDA MOCK-UP - Experimental results on turbulent heat transfer in mixed-convection for one large vertical heating cylinder in air cross-flow., *Turbulence, Heat and Mass Transfer (THMT06),* Dubrovnik, Croatia, September 25-29, 2006

[2] Archambeau, Fr., Méchitoua, N., Sakiz, M. *Code_Saturne*: A Finite Volume Code for the Computation of Turbulent Incompressible Flows - Industrial Applications - *International Journal of Finite Volumes 2004 (electronic)*

[3] Benhamadouche, S., Bournaud, S., Duret, B., Clement, Ph., Lecocq, Y., Large Eddy Simulation of mixed convection around a vertical heated cylinder cooled by a cross-flow air circulation., 2006,, *Conference on Modelling Fluid Flow Conference on Modelling Fluid Flow (CMFF'06),* Budapest, Hungary, September 6-9, 2006

[4] Menter, F. R., Two-Equation Eddy-Viscosity Turbulence Models for Engineering Applications, *AIAA Journal,* Vol. 32 N°8, August 1994

[5] B. Duret, J.C. Bonnard, S. Bournaud: Mixed-Convection from a Bundle of Heating Cylinders in a Cross-Flow Air-Circulation. Experiment and Analysis, *5th International Conference on Heat Transfer, Fluid Mechanics and Thermodynamics (HEFAT2007),* Sun City, South Africa, 2007

[6] Chassaing, P., Turbulence en Mécanique des Fluides, *Ed. Cépaduès, Col. Polytech*.

[7] Ferziger, J.H., Peric, M., Computational Methods for Fluid Dynamics, *Springer, third edition (2002)*

8 Rie and Chow

[9] Rupp, I., Peniguel, Ch., Coupling Heat Conduction, Radiation and Convection in Complex Geometries, *Int Journal of Numerical Methods for Heat and Fluid Flow*, **9** (1999)

[10] Zukauskas, A., Heat Transfer From Tubes In Crossflow, *Advances In Heat Transfer*, 18, pp. 87-159, 1987

[11] Williamson, C.H.K., Vortex Dynamics In The Wake, *Annu. Rev. Fluid. Mech*., 28, pp. 477-539, 1996

[12] White, F.M., *Fluid Mechanics*, 2nd Edition, McGraw-Hill, New York, pp. 253–268, 1986

[13] Bournaud, S., Duret, B., Berthoux, M., Mixed-Convection from heating Tube Bundle in a cross-flow Air-Circulation. Experiment and Analysis, *NURETH-12*, Pittsburgh, Pennsylvania, U.S.A. September 30-October 4, 2007

[14] Lesieur, M., Turbulence in fluids, *Kluwers, Third edition*

[15] Pope, S., Turbulent Flows, *Cambridge University Press*

[16] Jones, W. P. and Launder, B. E., The prediction of laminarization with a two-equation model of turbulence. Intl J. Heat Mass Transfer, 15:301-314, 1972.

[17] Speziale, C. G., Sarkar, S. and Gatski, T. B. Modeling the pressure-strain correlation of turbulence: an invariant dynamical system approach. J. Fluid Mech., 227:245--272, 1991.